# EXPERIMENTAL INVESTIGATION OF FRACTURE TOUGHNESS, HARDNESS AND LOAD-INDENTATION DEPTH RESPONSE OF TI-64 USING VICKERS INDENTATION TECHNIQUE

Riaz Muhammad[1*], Naseer Ahmeda, Abdul Basit[2], Rizwan Alim Mufti[2]

**Abstract**

*Titanium alloys display the matchless blend of physical and mechanical properties which have made them appropriate for aerospace, chemical, and biomedical industries services. Preeminent strength-to-density ratio, reduced density, incomparable corrosion resistance and tremendous properties at elevated temperature are the main attribute of titanium alloys. These alloys also exhibit low modulus of elasticity, making it ideal for spring, body implant, dental fixtures and different sports equipment. Ti-64 accounting for more than 50 percent of titanium usage in today modern world high-tech industries subjected to various nature of cyclic loading. This study includes the experimental assessment of fracture toughness of Ti-64 using indentation technique which is easy and fast experimental techniques. For this purpose Vickers-indentation technique is employed to report the hardness followed by fracture toughness evaluation of the studied alloy using indentation energy model. The indentation method resulted a fracture toughness of the studied alloy with 14.5% when compared to the results obtained from strain dependent ductile damage model.*

**KEYWORDS**: *Finite element; Fracture toughness; Vickers Indentation; Ti-64; Indentation energy model;*

## INTRODUCTION

Titanium alloys have recognized itself as most important structural material having high specific-strength, low density, virtuous corrosion resistance and fracture toughness. They have been widely used in aerospace, biomedical, and military applications. Technologically, it is very important to investigate the mechanical performance of titanium and its alloys and to analyze the deformation behavior (Chen *et al.,,* 2008). Ti-64 the most commonly used material accounting for more than 50 percent of titanium usage branded as grade 5 alloy and compromises the unsurpassed all round show for varieties of weight reduction application in automotive, aerospace and marine equipment (Muhammad 2013, Muhammad *et al.,* 2013, Maurotto *et al.,* 2014).

Starting from crack, flaw and other impurities, fracture failure is the most important and challenging one in the evaluation of mechanical design in different industrial applications (Amiri *et al.,* 2014). Fracture toughness is the material property which tells how much material can resist the crack propagation. It is the very important parameter to assess the structural integrity of mechanical component at different load. There are various standard methods to determine the fracture toughness, such as ASTM standard E399 and E1820 (ASTME384). These criteria are quite complicated and tedious in term of fixture design and specimen requirements. They include destructive tests and cannot be used in the final components to assess the fracture-toughness. A nondestructive test therefore is very beneficial for industrial related applications where final component can be tested.

Indentation fracture technique is an alternate route to determine fracture toughness and other properties. It has an advantage over conventional methods that, it is non-destructive and do not have many limitations of specimen as compared to the conventional methods.

Various indentation techniques are used for this purpose and Vickers indentation technique is the most prominent and vastly used method across the globe. Different models of this technique are available for brittle and ductile materials. Most of previous work has been done on brittle materials, however ductile material has more complicated behavior and in order to determine the fracture toughness of ductile material further investigation is needed. Therefore, indentation behaviors of ductile material are the part of this study (Amiri *et al.,* 2014).

In recent years, a nanoindentation technique was used to study international fracture and ductile-brittle evolution in hard coatings (Bhattacharyya *et al.,* 2018). The

[1] *Mechanical Engineering Department, CECOS University of IT and Emerging Sciences, Peshawar, Pakistan.*
[2]*Department of Mechanical Engineering, PIEAS, Islamabad, Pakistan.*

obtained results showed multi-crack propagation in hard coating at higher penetration. The obtained results are useful for the mathematical framework of modulus and hardness variation in indentation process. Furthermore, Liu's and Zeng's methods were combined in (Su *et al.,* 2018) to get accurate approximation of elastic energy used for calculating the fracture toughness.

In this study indentation test is used to assess the Hardness and the fracture toughness of Ti-64. The technique used is established on the principal of continuum-damage-mechanics (CDM) and indentation energy to fracture model. Hardness value along with indentation depth is found at different loads and the response of force on indentation depth is analyzed.

The evaluation of fracture toughness is based on the energy required for fracture which is obtained from the information of displacement and load and therefore related to the macroscopic-quantities. Conversely, in this study fracture energy is attained by the deformation obtained in indentation. The obtained two parameters are associated through CDM philosophy and due to generation of voids beneath the indenter, elastic modulus degradation and void act at micro scale (Amiri *et al.,* 2014).

In indentation technique, pileup and sinkin, occurrence is the most challenging which can affect the contact-area between the indenter and can affect the mechanical properties of the studied materials. However, in the current work, Sina Amiri et al (Amiri *et al.,* 2014) model is used which is the simple model and does not account for this phenomenon.

**Theoretical Model**

**Effective Modulus identification**

Depth and force control modes were used to carried out indentation tests. The generalized shape of obtained indentation depth and load is presented in Figure 1. The power-law described the loading portion of the Figure 1 and can be represented by Eq. (1), recognized as the power-law technique, and is not be linear.

$$F = F_m \left( \frac{h - h_p}{h_m - h_p} \right)^m \quad (1)$$

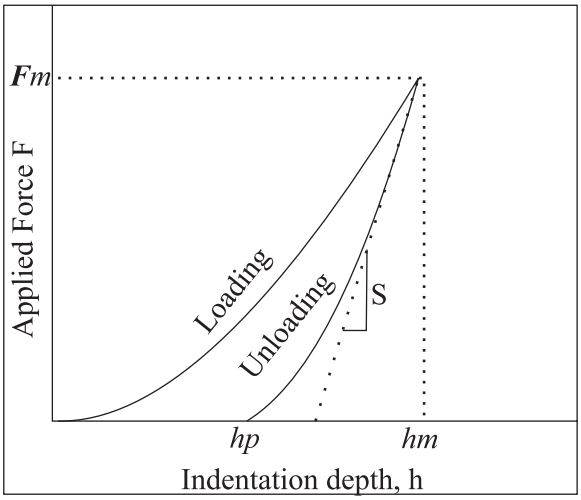


**Figure 1: Typical indentation load versus indentation depth curves**

where constant m can be gained by a curve fitting practice. To find out the effective and reduced modulus, contact stiffness is necessary which can be gauged by taking the derivative at peak-load.

Using the fundamental concept of contact mechanics, relations among the reduced modulus ($E_e$) of contact and modulus of elasticity of the two studied objects (Li *et al.,* 2015):

$$E_e = \left( \frac{1 - v_i^2}{E_i} + \frac{1 - v_j^2}{E_j} \right)^{-1} \quad (2)$$

Where

$v_i$ denote Poisson-ratio of the indenter, $v_j$ represent Poisson-ratio of the target specimen, $E_i$ symbolize indenter elastic modulus and $E_j$ is Elastic modulus of target specimen.

Similarly, reduced modulus $E_r$ can be expressed as (He *et al.,* 2011):

$$E_r = \left( \frac{k\sqrt{\pi}}{2\beta\sqrt{A_P}} \right) \quad (3)$$

Where

$k$ = measured stiffness at maximum depth during

unloading

$A_P$ = 24.50 $h_p^2$ = anticipated contact-area between material and indenter (Fischer-cripps 2011)

$\beta$ = constant =1 in case of Vickers indenter

**Indentation Energy Model**

Fracture failure happens when stress-intensity-factor (SIF) touches its critical limit at crack front additional detail about the model can be found in (Kumar and Prashant 2009). It can be expressed as

$$k_{1c} = \sqrt{2E\gamma} \quad (4)$$

Where $\gamma$ = surface energy per unit area and it can be expressed as:

$$\gamma = \int_0^{hp^*} \frac{P(h_p)}{A_p(h_p)} dh_p \quad (5)$$

Where limit of integration varies from 0 to $h_p^*$ which is the critical depth of indentation [6].

**Identification of Critical Indentation Depth**

For calculation of critical-fracture-toughness, critical depth of indentation is still obligatory. It is obvious that as critical depth increases, the modulus of elasticity underneath the indenter decreases non- linearly, hence, $h_p^*$ relates to critical damage Young's-modulus and can be calculated as mentioned in (He *et al.,* 2011). Using this $h_p^*$ critical surface-energy per unit area $\gamma^*$ can be calculated using Eq. (6), and finally fracture toughness is calculated using Eq. (5).

**Experimental Work**

**Grinding/ Polishing**

The studied alloy was cut into specimen of 1.5 cm x1 cm using EDM machine and were mounted in resin and epoxy solution to be held easily in the machine for grinding process. For preparation of mounting a mixture of Resin and Epoxy solutions is prepared with 60% Resin and 40% Epoxy (also called hardener). The samples were then embedded in an epoxy resin solution and allowed to cure overnight at room temperature. After that, samples were grinded and polished.

Water proof silicon carbide paper is used in the metallographic sample polishing machine with frequency convertor. Specimen is polished using different number of waterproof silicon carbide paper starting from coarse (180C) to fine (1000C). A light micrograph of the virgin sample is shown in Figure 2.

**Vickers-Indentation Tests**

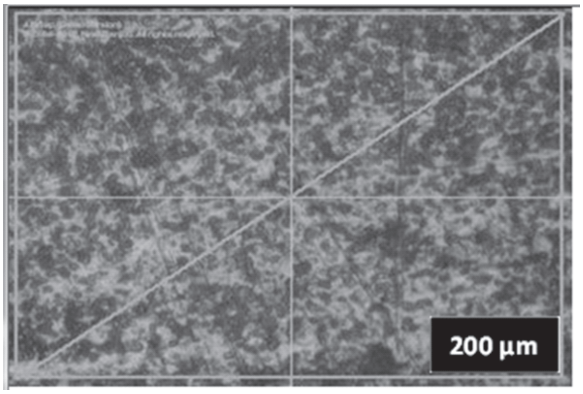


**Figure 2: Optical image (20 X) of Specimen before polishing as received.**

Vickers-indentation tests is performed in accordance with ASTM E384-99 (ASTME384) at different loading conditions. Figure 3 to Figure 5 shows the optical images of the indented area with different loading of Vickers impression.

**DISCUSSION ON RESULTS**

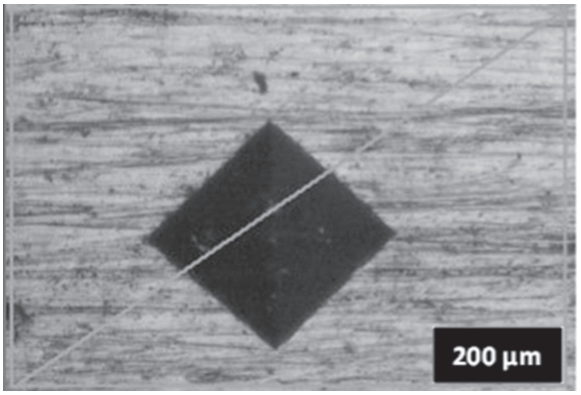


**Figure 3: Optical image of Vickers impression at 40 N.**

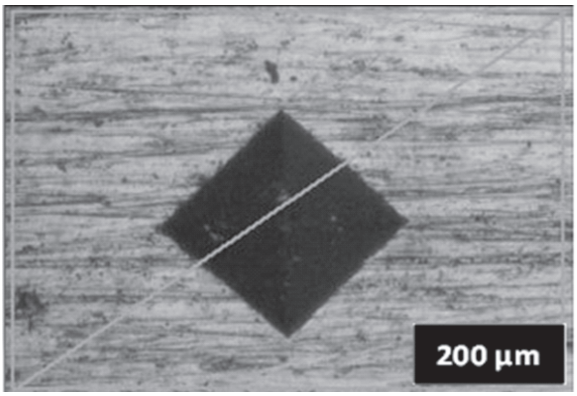


**Figure 4: Optical image of Vickers impression at 60 N.**

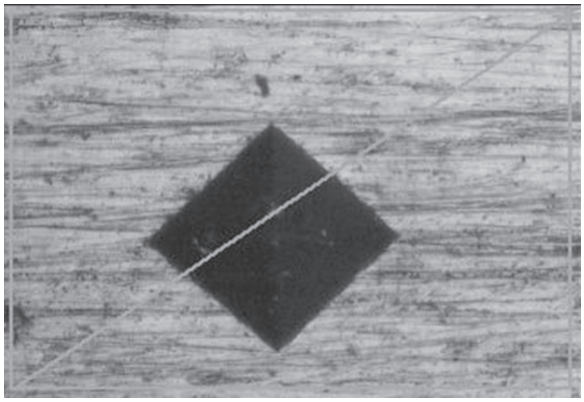

**Figure 5: Optical image of Vickers impression at 90 N**

### Effect of Indentation Load on Indentation Deformation

A Vernier caliper was used to measure the depth of indentation at various load conditions and is presented in Figure 6. The results demonstrated that indentation depth increases with an increase in load as expected. The results also show that variations of indentation depth are greater in smaller loads as compare to higher loads. As loads increases change in indentation depth decreases due to resistance offered by the materials and due to the strain hardening of the studied alloy. This is due to the fact that in start, to create and indent a higher stress is needed beneath the indenter, which causes greater dislocation in start of deformation or at smaller loads. The damage generation and accumulation beneath the indenter also decreases the elastic properties of material.

Dependence of Indenter's Tip Projected Area on Indentation Depth

The evaluation of indenter-tip projected area is necessary to determine the indentation energy, which is obligatory to find out the fracture-toughness of the studied alloy. Figure 7 shows all the experimental results of projected area of indenter and indentation deformation. By analyzing the results of Figure 7, it can be seen that Ap and hp shows the power-law relationship and can be expressed as:

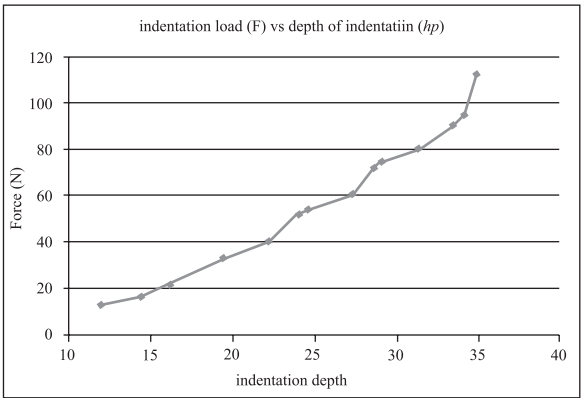


**Figure 6: Indentation depth and load during Vickers-indentation results**

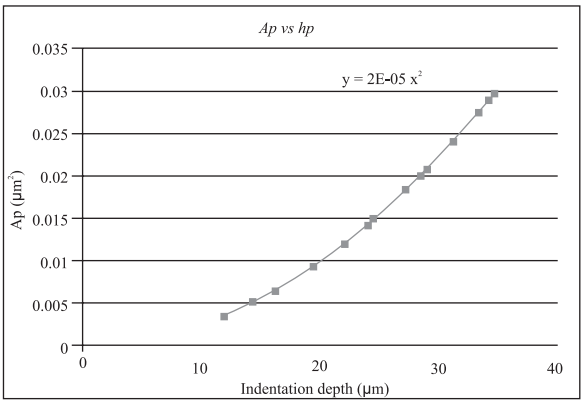


**Figure 7: Indentation depth and projected indentation-area**

$$d = kr^n \tag{7}$$

Comparing equ. 7 with the cure fitting equation from Figure 7, it can be shown that k = 2E-05 and n = 2.

Similarly, minimum projected area of indenter was

found to be 0.00352 μm2 at load of 12.74 N whereas maximum value of 0.02976 μm2 at a load of 112.7 N. Values of hp corresponding to the minimum and maximum projected area of indenters are 11.99 μm and 34.85 μm respectively.

Dependence of Average Diagonal Lengths of Indenter Impression on Indentation Load

The dependency of average diagonal-length of indenter on indentation load is described in a Figure 8. At every load five different readings of diagonal were taken and then average values of these five readings were used in this study. It can be seen that diagonal impressed length increases as the load increases. This is due to the fact that at higher loads, indenter penetration is more as compared to the lower loads which in turns create larger impressions of indenter in the material.

Average diagonal length of impression ranges from 84 μm to 244 μm corresponding to the available loads of 12.74 N to 112.7 N. This average diagonal impression values were used to find out the hardness values of Ti-64.

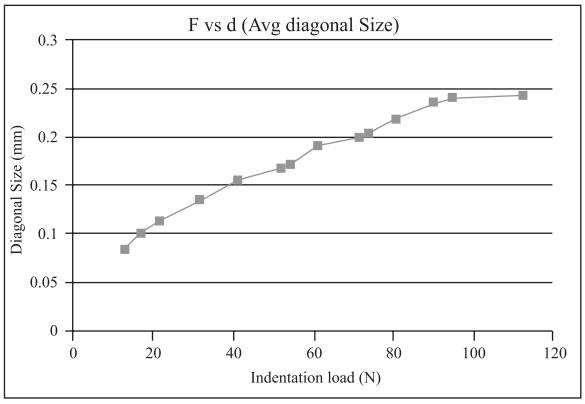


**Figure 8: Dependence of avg. diagonal length on indentation load**

**Indentation Hardness**

Rhombus like shapes along with the square shapes were recorded during the Vickers-indentation tests (Figure 3 to Figure 5) The occurrence of rhombus like outline depicts the anisotropic characteristic of hexagonal close-packed (hcp) arrangement of titanium atoms (Chen *et al.,* 2008). It was also observed that the residual impression of indentation is a function of indention depth and higher diagonal size was recorded at higher penetration.

Figure 9 shows the dependence of Vickers hardness on the applied indentation loads. The results of indentation hardness shows evidence that the indentation hardness values obtained from the Vickers indentation test decreases slightly from 3.5 to 3 GPa . The average value of hardness comes out to be 3.20 GPa in this study which is in good agreement with (Poondla *et al.,* 2009) with maximum error of 1.25%. So results obtained from the experiments are good enough for further analysis.

As mentioned previously that hardness value slightly drops from 3.5 to 3 GPa is due to the indentation size effect (ISE). At higher loads, hardness value does not change and almost remain same however at lower loads slightly changed in hardness values were observed. It was also observed that at higher loads indentation depth is more and hardness values differs slightly at smaller loads so due to ISE hardness value slightly changes.

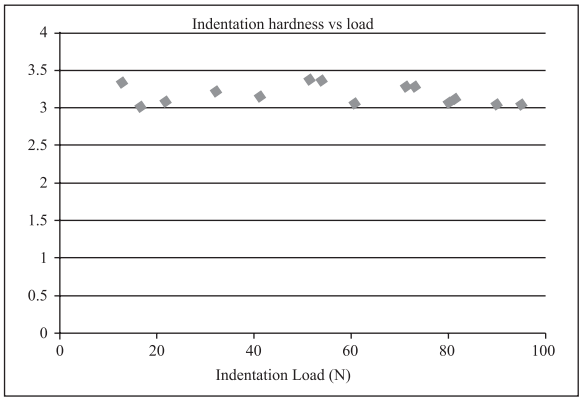


**Figure 9: Measured hardness for studied alloy**

Effect of Indentation Depth (hp) on Indentation Elastic Modulus

Indentation elastic modulus and its relationship with the indentation depth is necessary for assessment of the critical indentation depth which can lead us to assess the fracture toughness.

For damage accumulation and growth generally young's modulus is characterized. Due to accumulation of dislocations stress concentration may occur and it can easily cross the critical value of stress in indentation process. Hence, generation and accumulation of damage occurs which decreases the elastic properties and in turns young's modulus decreases. In brittle material

these dislocation may completely go forward in to the micro cracks but in ductile material these dislocation can incorporate into a cavity-dislocation and may not spread instantly (He *et al.,* 2011, Dong *et al.,* 2013, Khan *et al.,* 2018).

Figure 10 shows the relationship between the indentation elastic modulus (also called as damage modulus) and the indentation depth. The damage modulus decreases with increase in the indentation depth, exponentially. Moreover, it can be found that rapid decreases in ED was seen at lower loads, however at higher loads its variation is negligible. To be more specific, ED drops down rapidly from load of 12 N to 40 N and remains almost same at higher loads ranging from 40 N to 112 N.

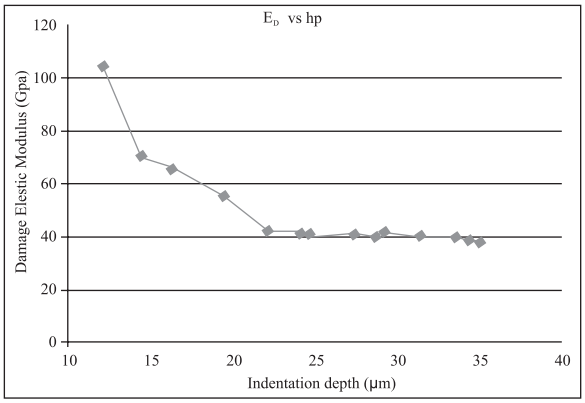


**Figure 10: Damaged elastic modulus effect with indentation depth**

Similarly, corresponding values of indentation depths ranges from 12 μm to 22 μm and 22 μm to 33.84 μm, respectively. The value of ED rapidly decreases from indentation depth of almost 12 μm to 22 μm and remains same from 22 μm to onward.

The decrease in ED is due to the micro defects and cracks generated underneath the indenter once the indenter applied load reached to the damaged threshold value (Dong *et al.,* 2013). Consequently, it can be established that during experiments increase in damage caused by the hoarded dislocation could be explained this decrease in the indenation modulus. In the start of deformation, dislocations are more so higher stress is generated beneath the indenter which can cross the threshold value of stress in indentation process. The damgae during this process accumulate very fast and due to this reason ED decrease rapidly.

At higher load with increase in indentation depth accumulation density decrease rapidly with loads and remains same at high loads. Therefore at the end of deformation accumulation density is very small and remains constant therefore ED doses not changes and remains same at higher loads of 112.7 N (Dong *et al.,* 2013).

**Fracture Toughness Measurement**

To find out the fracture toughness critical indentation depth was first identified by using the method already explained in section 2.1 and using ED and hp curve and it comes out to be 16 μm.

By using this critical indentation depth and using Eq. (5) and Eq. (6), fracture toughness values was calculated which are shown in the Figure 11.

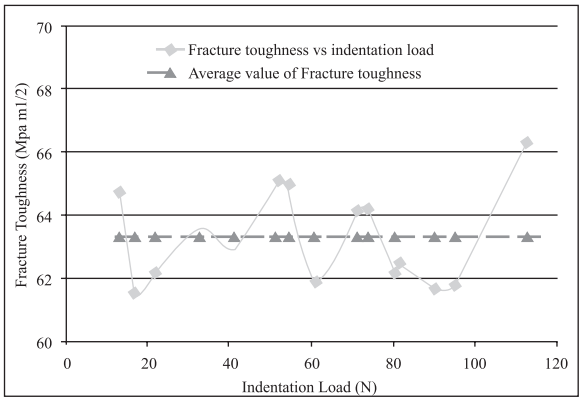


**Figure 11: Calculated fracture toughness value of the studied alloy at various load**

It can be seen in Figure 11 that with indentation load fracture toughness values varies from 61.66 MPa m1/2 to 66.32 MPa m1/2 . The average value of fracture toughness comes out to be 63.35 MPa- m1/2.

Jinghui Li et al (Li *et al.,* 2015) in his experiments using strain dependent ductile damage model found that maximum value of fracture toughness of Ti-64 comes out to be 77.75 MPa- m1/2 . So the relative difference with this method is 14.7 % .

**CONCLUSIONS**

The main conclusions of the current work is summarized below:

The hardness value of Ti-64 ranges from 3 to 3.5 GPa which shows that Ti-64 is a very tough and hard material and it shows a lot of resistance to the indentation.

The indentation method is easy compared to other tedious methods and gives us fracture toughness values with percent error of 14.5% when compared to strain dependent ductile damage model.

Average fracture toughness values of Ti-64 was found to be around 63 MPa m1/2 which is quiet large value as compared to many other alloys, so it shows that Ti-64 also offer great resistance to the fracture.

The usage of Ti-64 in the turbine blade can also increase the efficiency of gas turbine.

## REFERENCES


1. *Amiri, S., N. Lecis, A. Manes and M. J. M. R. C. Giglio (2014), "A study of a micro-indentation technique for estimating the fracture toughness of Al6061-T6", Vol 58: pp. 10-16.*

2. *ASTME384 Standard test method for microindentation hardness of materials1. 99e1.*

3. *Bhattacharyya, A., R. Kumar, S. Priyadarshi, S. Shivam, S. J. J. o. M. E. Anshu and Performance (2018), "Nanoindentation Stress–Strain for Fracture Analysis and Computational Modeling for Hardness and Modulus", pp. 1-8.*

4. *Chen, R., F. Yang, M. A. Imam, C. Feng and P. J. J. o. M. R. Pao (2008), "Microindentation of titanium: Dependence of plastic energy on the indentation depth and time-dependent plastic deformation", Vol 23(4): pp. 1068-1075.*

5. *Dong, J., F. Li, C. J. M. S. Wang and E. A (2013), "Micromechanical behavior study of α phase with different morphologies of Ti–6Al–4V alloy by microindentation", Vol 580:pp. 105-113.*

6. *Fischer-cripps (2011), Nanoindentation Testing.*

7. *He, M., F. Li, J. Cai, B. J. T. Chen and A. F. Mechanics (2011), "An indentation technique for estimating the energy density as fracture toughness with Berkovich indenter for ductile bulk materials", Vol 56(2): pp. 104-111.*

8. *Khan, M. I., A. Shakoor, K. Azam, M. Habib, R. Muhammad, S. A. Shah, A. J. P. S. Khan and Technology (2018), "Experimental and numerical analysis of nanoindentation of Ti-6246 alloy", Vol 36(4):pp. 408-418.*

9. *Kumar, P. and K. Prashant (2009), Elements of fracture mechanics, Tata McGraw-Hill Education.*

10. *Li, J., F. Li, X. Ma, Q. Wang, J. Dong and Z. Yuan (2015), "A strain-dependent ductile damage model and its application in the derivation of fracture toughness by micro-indentation", Materials and Design 67(Complete): pp. 623-630.*

11. *Maurotto, A., C. Siemers, R. Muhammad, A. Roy, V. J. M. Silberschmidt and M. T. A (2014), "Ti alloy with enhanced machinability in UAT turning", Vol 45(6):pp. 2768-2775.*

12. *Muhammad, R. (2013), "Hot ultrasonically assisted turning of Ti-15V3Al3Cr3Sn: experimental and numerical analysis", © Riaz Muhammad.*

13. *Muhammad, R., M. Demiral, A. Roy and V. Silberschmidt (2013), "Modelling the dynamic behaviour of hard-to-cut alloys under conditions of vibro-impact cutting", Journal of Physics: Conference Series, IOP Publishing.*

14. *Poondla, N., T. S. Srivatsan, A. Patnaik, M. J. J. o. A. Petraroli and Compounds (2009), "A study of the microstructure and hardness of two titanium alloys: Commercially pure and Ti–6Al–4V", Vol 486(1-2):pp. 162-167.*

15. *Su, X., P. Chen and T. J. P. Ma (2018), "Evaluation of shale fracture toughness based on micrometer indentation test", Petroleum https://doi.org/10.1016/j.petlm.2018.05.005.*